Distinct duration and diet dependent lipid profiles and renal complications in GCK-MODY

Yadi Huang[1,#], Yuxin Fan[1,#], Yang Liu[1,#], Xuan Liu[1], Wei Li[1], Ying Yang[1], Ziyue Zhang[1], Shifeng Ma[1], Shuhui Ji[1], Shanshan Chen[1], Hua Shu[1], Wenli Feng[1], Kunlin Wang[1], Qing He[1], Wenjun Qi[2], Yu Fan[1,‡], Xin Li[1,‡], Ming Liu[1,‡]

[1]Department of Endocrinology and Metabolism, Tianjin Medical University General Hospital, Tianjin, 300052, China

[2]NHC Key Laboratory of Hormones and Development, Chu Hsien-I Memorial Hospital and Institute of Endocrinology, Tianjin Medical University, Tianjin, 300134, China

[#]Authors contribute equally to the work.

[‡]To whom correspondence may be addressed. Ming Liu, Department of Endocrinology and Metabolism, Tianjin Medical University General Hospital, #154 Anshan Road, Heping District, Tianjin, 300052, China. Email: mingliu@tmu.edu.cn; Yu Fan, Email: fanyu5@hotmail.com; Xin Li, email: lixin920616@163.com.

Corresponding author:

Ming Liu[1,‡] M.D., Ph.D.

Email: mingliu@tmu.edu.cn

Tel: +86-22-60817182

Address: Department of Endocrinology and Metabolism, Tianjin Medical University General Hospital, 154 Anshan Road, Heping District, Tianjin, China 300052

Distinct duration and diet dependent lipid profiles and renal complications in GCK-MODY

Yadi Huang[1,#], Yuxin Fan[1,#], Yang Liu[1,#], Xuan Liu[1], Wei Li[1], Ying Yang[1], Ziyue Zhang[1], Shifeng Ma[1], Shuhui Ji[1], Shanshan Chen[1], Hua Shu[1], Wenli Feng[1], Kunlin Wang[1], Qing He[1], Wenjun Qi[2], Yu Fan[1,‡], Xin Li[1,‡], Ming Liu[1,‡]

Abstract

Heterozygous inactivating mutations in the glucokinase (GCK) gene cause one of the most common types of maturity-onset diabetes of the young type 2 (MODY2), also named GCK-MODY. Studies suggest that, unlike other types of diabetes, patients with GCK-MODY do not have increased risk of diabetic complications and therefore do not typically require antihyperglycemic therapy. However, long-term outcomes of GCK-MODY on lipid profiles and chronic complications remain unclear. Herein, using a knock-in mouse model expressing a novel MODY causing mutation GCK-Q26L (GCK^{Mut}), we examined age- and diet-related lipid profiles and diabetic complications. We found that, although GCK^{Mut} mice exhibited mild elevated blood glucose, the lipid profiles, body fat composition, and diabetic kidney disease (DKD) were initially improved in high-fat-diet (HFD) fed mice at the age of 28 weeks, supporting potential beneficial effects of GCK^{Mut} on lipid metabolism and kidney health. Unexpectedly however, those protective effects diminished by 40 weeks, and became more severe dyslipidemia and kidney injury associated with renal fibrosis and inflammation at 60-week-old mice fed with normal diet (ND) or HFD. Those findings revealed distinct duration- and diet-dependent effects

of inactivating GCK mutation on lipid profiles and DKD, highlighting previously unrealized long-term chronic complications in GCK-MODY.

Keywords: Glucokinase, GCK-MODY, Lipid profiles, Diabetic kidney disease

69 **1. Introduction**

70 Glucokinase (GCK), a glycolytic enzyme belonging to the hexokinase family, plays a pivotal
71 role in catalyzing the conversion of glucose into glucose-6-phosphate, a primary step in glucose
72 metabolism within pancreatic β-cells and hepatocytes [1-3]. Heterozygous inactivating mutations
73 in the GCK gene cause maturity-onset diabetes of the young type 2 (MODY2, also named GCK-
74 MODY), which is one of the most common types of monogenic diabetes [4-6]. Patients with
75 GCK-MODY typically present mild to moderate non-progressive elevated fasting blood glucose
76 (FBG) without significant abnormalities or even improvement of lipid metabolism [7, 8]. More
77 importantly, current evidence indicates that individuals with GCK-MODY are not associated
78 with increased risks of chronic diabetic complications compared to the other types of diabetes [9].
79 Therefore, current consensuses suggest that such patients may not necessitate pharmacological
80 interventions [10, 11].

81

82 However, due to the limited number of patients diagnosed with GCK-MODY, the perspective
83 interventional or observational studies focusing long-term outcomes of GCK-MODY are scarce.
84 Additionally, given the potential impact of persistent hyperglycemia on ocular, vascular,
85 neurological and renal diseases [12-15], it is important to investigate long-term effects of
86 inactivating GCK mutations on lipid metabolism and functional and structural alterations in
87 microvascular complications associated with prolonged hyperglycemia.

88

89 Recently, we have established a knock-in mouse line expressing a novel GCK mutation (GCK-
90 Q26L, GCK^{Mut}) identified in two members of a family with early onset diabetes, and
91 demonstrated that this mutation indeed impaired insulin secretion causing mild elevated FBG

92 and impaired glucose tolerance that mirrors the phenotypes of patients with GCK-MODY
93 (https://doi.org/10.1101/2024.08.13.24311668). In this study, using this knock-in mouse model,
94 we examined age- and diet-related lipid profiles and diabetic complications in the GCK-MODY.
95 We found that GCK mutant indeed presented beneficial effects on lipid metabolism, body fat
96 composition, and renal injury in high-fat-diet (HFD) fed GCK^{Mut} mice at the age of 28 weeks.
97 However, those protective effects diminished with time, and more severe dyslipidemia and
98 kidney injury associated with renal fibrosis and inflammation were observed in GCK^{Mut} mice fed
99 with HFD at the age of 60 weeks. Those findings revealed distinct duration- and diet-dependent
100 effects of inactivating GCK mutation on body composition, lipid profiles, and diabetic kidney
101 disease (DKD), highlighting previously unrealized long-term metabolic abnormalities and
102 chronic diabetes complications in GCK-MODY. This is poised to offer valuable insights for the
103 prevention and treatment of individuals diagnosed with GCK-MODY aiming to improve long-
104 term reduction of chronic complications. Given the fact that decreased expression and function
105 of GCK are also seen in type 2 diabetes [16], this study may also have clinical implications in the
106 management of type 2 diabetes (T2D).
107

108 **2. Methods and Materials**

109 **2.1 Animal models**

110 Male WT mice were purchased from SPF Biotechnology, while a global GCK-Q26L (GCK^{Mut})
111 knock-in mouse line was established as described in our previous study. Both GCK^{Mut} mice and
112 WT mice were housed in pathogen-free conditions within the the Laboratory Animal Center of
113 Tianjin Medical University Chu Hsien-I Memorial Hospital. WT and GCK^{Mut} male mice were
114 randomly assigned to four groups and subjected to either a normal diet (ND; comprising 20%

115 protein, 4% fat, 5% fiber, SCXK(LU) 2018-0003) or a high-fat diet (HFD; comprising 20%
116 protein, 60% fat, 20% carbohydrates, D12492, Research Diets) from four weeks of age until they
117 reached 28, 40, and 60 weeks of age. Throughout this period, monitoring of body weight and
118 blood glucose levels was conducted every 4 weeks. All mice utilized in the study were
119 maintained on a C57BL/6J background and housed in a 12 h light/dark cycle in a temperature
120 (22–25 °C) and humidity (55 ± 5%) control room.
121

122 **2.2 Biochemical measurements**

123 Blood glucose levels were assessed using an automated glucometer (Roche, ACCU-CHEK,
124 Germany). Mice were placed in metabolic cages to collect 24-hour urine samples. Various
125 parameters including serum total cholesterol (TC), triglycerides (TG), low-density lipoprotein
126 cholesterol (LDL-c), high-density lipoprotein cholesterol (HDL-c), serum creatinine, 24-hour
127 urinary albumin excretion (UAE), and urinary creatinine were determined by kits provided from
128 Nanjing Jiancheng Institute of Bioengineering (Nanjing, China).
129

130 **2.3 Intraperitoneal glucose tolerance test and insulin tolerance test**

131 The intraperitoneal glucose tolerance test (IPGTT) involved the intraperitoneal administration of
132 1 g/kg body weight of glucose in mice following a 6-hour fasting period. The area under the
133 curve (AUC) was determined using the trapezoidal rule. Simultaneously, blood samples collected
134 at each time point were utilized to measure blood glucose and serum insulin levels employing an
135 insulin ELISA assay kit (EZassay, China), following the manufacturer's instructions. For the
136 intraperitoneal insulin tolerance test (IPITT), mice that fasted for 4 hours received an
137 intraperitoneal injection of 0.75 U/kg body weight of insulin. Tail vein glucose levels were

138 monitored at 0, 15, 30, 60 and 120 minutes post-injection. All experiments mentioned above
139 were conducted using age- and sex-matched cohorts.
140
141 **2.4 Body composition measurements**
142 Fat mass of was measured using a Bruker Minispec mq7.5 (Brucker).
143
144 **2.5 Histologic evaluation and transmission electron microscopy anslysis**
145 Following anesthesia, mice were euthanized subsequently the kidneys were harvested， which
146 were fixed in 4% paraformaldehyde, then paraffin-embedded and were cut into 5-μm-thick
147 sections. Subsequently, these sections were stained, and after sealing with neutral balsam, images
148 were captured using AxioImagerM2 (Carl Zeiss, Oberkochen, Germany). The extent of kidney
149 injury within each group was assessed utilizing Image-ProPlus 6.0 software. The sections
150 underwent staining procedures involving hematoxylin and eosin (H&E), Periodic acid-Schiff's
151 (PAS), and Masson's trichrome. For semi-quantitative analysis, twenty stained glomeruli per
152 section were randomly chosen (5 mice per group) for analyses. For transmission electron
153 microscopy (TEM), fresh isolated kidney tissues were sliced into small pieces and then fixed in
154 2.5% glutaraldehyde for a duration of 12 hours. Subsequently, the tissues underwent treatment
155 with 1% osmium tetroxide. Ultrathin sections were obtained utilizing an ultramicrotome
156 (LeicaEMUC7, Germany), followed by a dehydration process using gradient alcohol,
157 permeabilization with acetone, and final embedding in epoxy. The obtained ultrathin sections,
158 measuring between 70-90 nm, were stained with uranyl acetate and lead citrate. These sections
159 were examined using a transmission electron microscope (TEM) (HT7700, Japan).
160

161 **2.6 RNA Extraction, cDNA Synthesis, and Quantitative real-time PCR (qRT-PCR)**

162 Total RNA was extracted and purified from renal tissues using TRIzol reagent (Invitrogen, USA).
163 Subsequently, cDNA was synthesized utilizing the PrimeScriptTM RT kit with gDNAEraser
164 (Takara, Japan), following the manufacturer's instructions. qRT-PCR assays were conducted in a
165 20 μL reaction volume employing TB Green Premix Ex Taq^{TM} (Tli RNaseH Plus) (Takara,
166 Japan). GAPDH served as the internal control. The primers utilized in this study were designed
167 and chemically synthesized by ZTSINGKE Biological Technology (Beijing, China) Co. Ltd.
168 Details of the primer sequences were provided in **Supplemental Table S1**.

169

170 **2.7 Protein Extraction and Western Blot Analysis**

171 Renal tissues were lysed using RIPA lysis buffer for protein extraction. Protein samples were
172 then loaded onto SDS-PAGE, electrophoretically separated, and subsequently transferred to
173 nitrocellulose membranes. These membranes were blocked using 5% skimmed milk followed by
174 blotted with indicated antibodies, and visualized by enhanced chemiluminescence (CLiNX,
175 Shanghai, China). The following antibodies were utilized in this study: anti-E-Cadherin (A3044;
176 ABclonal), anti-Vimentin (A11423; ABclonal), anti-α-SMA (A7248; ABclonal), anti-IL-1β
177 (A16288; ABclonal), anti-TNF-α (A11534; ABclonal), and anti-β-actin (KM9001T, Sungene).

178

179 **2.8 Transcriptome analysis**

180 Renal transcriptome analysis was conducted by BGI Group, encompassing RNA extraction,
181 library preparation, and sequencing. Data processing adhered to the standard BGI mRNA
182 analysis pipeline. Statistical analysis was executed utilizing the Deseq2 software package
183 (v1.28.1). Differentially expressed genes (DEGs) were identified using a threshold of log2 (fold

184 change) absolute value ≥ 1 and false discovery rate ≤ 0.05. For further insights, Gene
185 Ontology (GO) analysis was carried out using cluster/profiler (v3.16.1). Pathway visualization
186 was accomplished using GraphPad Prism 8.
187
188 **2.9 Statistics**
189 Statistical analyses were conducted utilizing GraphPad Prism 8 software. The data are presented
190 as mean ± standard deviation. Analysis involved unpaired Student's t-tests, with statistical
191 significance set at the traditional critical value of $P < 0.05$. Each experiment was independently
192 repeated at least three times.
193
194 **3. Results**
195 **3.1 GCK^{Mut} impairs insulin secretion leading to elevated FBG but improves lipid profiles**
196 **without affecting body fat composition in mice fed with normal diet (ND)**
197 We have monitored body weight (BW) and FBG of ND fed mice every 4 weeks until 60 weeks
198 of age, and found that GCK^{Mut} caused non-progressively mild elevated FBG without affecting
199 BW (**Fig. 1A-B**). To evaluate the effect of GCK^{Mut} on insulin secretion and glucose tolerance,
200 we performed intraperitoneal glucose tolerance tests (IPGTT) at the ages of 28, 40, and 60 weeks,
201 respectively. We found that GCK^{Mut} resulted in impaired glucose tolerance associated (**Fig. 1C-E,**
202 **Fig. S1A-C**) with decreased basal and glucose stimulated insulin secretion (**Fig. 1F-H, Fig.**
203 **S1D-F**). However, GCK^{Mut} did not appeared to affect insulin sensitivity during intraperitoneal
204 insulin tolerance tests (IPITT) (**Fig. 1I-K, Fig. S1G-I**). Next, we examined body composition
205 and lipid profiles of GCK^{Mut} mice, and found that although GCK^{Mut} did not change the body fat
206 composition, the weight of perirenal white adipose tissue (pWAT), and the weight of gonadal

207 white adipose tissue (gWAT) (**Fig. 1L-N**), it indeed decreased levels of serum triglyceride (TG)
208 and low-density protein cholesterol (LDL-c) in 28-week-old mice. However, those beneficial
209 effects on lipid metabolism diminished at 40 and 60 weeks of age (**Fig. 1O-R**). Those data
210 demonstrate that decreased activity of GCK causes mild non-progressive hyperglycemia with
211 improved lipid profiles at young age and this improvement waned over time.
212

213 **3.2 Exacerbation of proteinuria and renal pathological changes in 60-week-old GCK^{Mut}**
214 **mice fed with ND**

215 Hyperglycemia is associated with microvascular complications in patients with T2D [17, 18].
216 Given the fact that persistent elevated blood glucose in patients with GCK-MODY, it is
217 important to determine the long-term effects of GCK-MODY on chronic diabetes complications.
218 We therefore measured kidney weight (KW) and BW and found no significant difference in the
219 KW/BW ratio between GCK^{Mut} and control mice at 28, 40, and 60 weeks of age (**Fig. 2A**).
220 Additionally, in comparison to WT mice, GCK^{Mut} mice displayed no differences in the levels of
221 24-hour urinary albumin excretion (UAE), urinary albumin-to-creatinine ratio (UACR), and
222 serum creatinine at 28 and 40 weeks of age. However, UAE, UACR, and serum creatinine were
223 notably increased at 60 weeks of age in GCK^{mut} mice (**Fig. 2B-D**). Histological analyses
224 demonstrated relatively normal glomerular and tubular morphology and structure in GCK^{Mut}
225 mice at 28 and 40 weeks of age. PAS and Masson staining indicated marginal differences in
226 thylakoid dilation and renal fibrosis between GCK^{Mut} and control mice at 28 and 40 weeks,
227 which exacerbated notably at 60 weeks of age (**Fig. 2E-G and K-L**). Subsequently, we utilized
228 transmission electron microscopy to examine glomerular structure at 28, 40, and 60 weeks of age
229 in both groups of mice. The observations indicated a trend of increased thickness of glomerular

230 basement membrane (GBM) at 28 and 40 weeks of age, and a significant thickening of GBM
231 was evident at 60 weeks of age in GCK^{Mut} mice (**Fig. 2H-J and M**).
232

233 **3.3 Renal fibrosis- and inflammation-associated genes exhibit high expression in aging**
234 **GCK^{Mut} mice fed with ND**

235 To investigate pathways involved in long-term renal changes in GCK^{mut} mice, we performed
236 transcriptome analysis using kidneys from littermate controls and GCK^{Mut} mice. Gene Ontology
237 (GO) analysis of the two groups of mice at 60-week-old age revealed that the 940 differentially
238 expressed genes (DEGs, with $|Log2|$ fold change ≥ 1 and false discovery rate ≤ 0.05), which
239 were primarily enriched in collagen fibril organization, cell-matrix adhesion, and inflammatory
240 response (**Fig. 3A**), consistent with previous reports indicating that excessive accumulation of
241 extracellular mesenchymal tissue and pro-inflammatory responses contribute to the progression
242 of DKD [19-21]. We further analyzed the DEGs involved in biological progression of DKD, and
243 found that Vim (Vimentins, encoding intermediate filaments), Acta2 (α-SMA, encoding alpha-
244 smooth muscle actin), Col1a1 (COL1A1, encoding type I collagen) and Tnf exhibited significant
245 up-regulation in GCK^{Mut} mice at 60 weeks of age (**Fig. 3B**). The changes of the these genes were
246 further confirmed by quantitative real-time PCR (qRT-PCR) excepted Colla1 that did not show a
247 statistic difference between two groups. The gene Cdh1 (cadherin 1, encoding E-cadherin),
248 which maintains stable cellular connections and cellular architecture integrity [22], was
249 significantly downregulated (**Fig. 3C**). Furthermore, Western blot analysis verified that the
250 protein levels of Vim, α-SMA, TNF-α and IL-1β were indeed significantly elevated in the
251 kidneys of 60-week-old GCK^{Mut} mice, whereas no significant changes in proteins levels and
252 mRNA levels were observed in 28- and 40-week-old mice (**Fig. 3D-G, Fig. S2**). These results

253 suggest that upregulation of the genes associated with renal fibrotic and inflammatory responses
254 may be attributed to long-term kidney injury in the old GCK^{mut} mice.
255

256 **3.4 The body composition and lipid profile of 28-week-old GCK^{Mut} mice fed with HFD**
257 **improved, but these improvements disappeared at 40 weeks and worsened further at 60**
258 **weeks**

259 A recent study has revealed that partial inactivation of GCK can yield beneficial effects on
260 hepatic lipid metabolism and inflammation [23]. These effects have been postulated as a
261 potential rationale behind the favorable lipid profile and reduced cardiovascular risk observed in
262 patients with GCK-MODY [24, 25]. Our data indicated that although improved circulating lipid
263 profiles were indeed validated at early time in GCK^{Mut} mutant mice, those improvements
264 diminished over the time in mice fed with ND (**Fig. 1O-R**). We therefore asked what effects of
265 additional metabolic stress inactivation of GCK on glucolipid metabolism and renal injury. We
266 randomly grouped 4-week-old littermate mutant and control mice for the HFD regimen while
267 maintaining the same experimental protocols as those used for mice fed with ND. Our findings
268 revealed a transient small but statistic decrease in body weight in 28-week-old GCK^{Mut} mice fed
269 with HFD. However, this divergence disappeared in the mice fed with HFD till 40- and 60-week-
270 old (**Fig. 4A**). Additionally, elevated fasting and postprandial blood glucose (**Fig. 4B-E, Fig.**
271 **S3A-C**), decreased circulating insulin (**Figs. 4F-H, Fig. S3D-F**), and insulin sensitivity (**Figs. 4I-**
272 **K, Fig. S3G-I**) had all similar trends as that we observed in mice fed with ND. These data
273 further demonstrate that although elevated FBG and impaired glucose intolerance persist, these
274 diabetes phenotypes are stable and are not aggravated even under HFD in GCK^{mut} mice.
275

276 Next, we analyzed body composition and revealed a significant reduction in fat mass in HFD fed
277 GCK^{Mut} mice at 28 weeks in comparison to the control group (**Fig. 4L**). Similarly, pWAT and
278 gWAT (**Fig. 4M-N**) as well as serum TC and LDL-c levels displayed noteworthy reductions
279 along with elevated HDL-c in HFD fed GCK^{Mut} mice at 28 weeks (**Fig. 4O-R**). However, at 40
280 to 60 weeks of age, the aforementioned indices were progressively worse, resulting in significant
281 deleterious changes of lipid profiles at the age of 60 weeks (**Fig. 4S-V**). These data suggest that
282 long-term exposure of hyperglycemia and HFD may override the potential beneficial effects of
283 GCK^{Mut} on lipid metabolism and body composition, manifesting more severe metabolism
284 disorders.
285

286 **3.5 GCK^{Mut} attenuates HFD induced renal injury at 28 weeks of age, but aggravates renal**
287 **injury at 60 weeks of age**

288 Previous study has indicated that ectopic lipid accumulation in the kidneys contributes to kidney
289 injury [26-28]. Analogous to alterations in lipid profiles, quantitative analysis of lipids extracted
290 from kidneys exhibited significantly reduced TC and TG levels along with decreased kidney
291 weight in GCK^{Mut} mice fed with HFD at the age of 28 weeks. However, with extended exposure
292 to the hyperglycemia and HFD, TC and TG contents in the kidneys of GCK^{Mut} mice gradually
293 increased in comparison to WT mice over time (**Fig. 5A-C, Fig. S4A-B**). To further evaluate
294 renal damage, we also examined 24-hour UAE, UACR, and serum creatinine levels in both
295 groups of mice. The findings revealed reduced UAE, UACR, and serum creatinine levels in
296 GCK^{Mut} mice fed with HFD at the age of 28 weeks, but increased alterations in 60-week-old
297 HFD fed GCK^{Mut} mice (**Fig. 5D-F, Fig. S4C-E**). Notably, histological staining indicated
298 significantly reduced renal mesangial matrix and collagen fiber deposition in GCK^{Mut} mice

299 compared to WT mice fed with HFD at the age of 28 weeks, but these indicators gradually
300 increased at 40 and 60 weeks (**Fig. 5G-I and M-N**). Furthermore, TEM analysis demonstrated a
301 significantly smaller degree of GBM thickness in GCK^{Mut} mice at 28 weeks compared to control
302 mice. However, this thickness significantly increased at 60 weeks (**Fig. 5J-L and O**). These
303 findings indicate that proteinuria progression and pathological damage induced by a HFD were
304 mitigated in GCK^{Mut} mice fed with HFD at early age, whereas long-term (60 weeks) HFD and
305 hyperglycemia worsened renal damage at 60 weeks in GCK^{mut} mice. Altogether, those findings
306 highlight distinct diet and duration dependent effects of GCK inactivating mutation on lipid
307 profiles and the kidney.
308

309 **3.6 GCK^{mut} attenuates the expression of genes associated with renal fibrosis and**
310 **inflammation in 28-week-old HFD fed mice, whereas reversal effects GCK^{mut} on the**
311 **changes of above genes are observed after long-term HFD exposure**

312 To investigate the mechanism of attenuated renal injury in GCK^{Mut} induced by HFD, we
313 conducted transcriptome analyses of renal samples from GCK^{Mut} mice fed with HFD at the age
314 of 28 weeks. GO enrichment analysis revealed that 462 DEGs were predominantly involved in
315 fatty acid metabolic process, extracellular matrix organization, immune system process, cell-
316 matrix adhesion, collagen fibril organization and inflammatory response (**Fig. 6A).** Further
317 analysis of genes enriched in GO highlighted that fibrosis-related genes such as Col1a1 and Vim,
318 and inflammatory cytokines like Tnf were significantly down-regulated. Additionally, genes
319 associated with lipid catabolic process, such as Ppara and Lpl, displayed significant up-
320 regulation (**Fig. 6B).** Subsequently, qRT-PCR confirmed that mRNA levels of Vim, Tnf were
321 significantly reduced and Cdh1, Ppara, whereas Lpl were significantly elevated in the kidneys of

322 GCK^{Mut} mice compared with WT mice (**Fig. 6C**). Western blot also showed that the expression
323 of E-Cadherin was increased, whereas the expression of Vim , α-SMA and TNF-α were
324 decreased in GCK^{Mut} mice fed with HFD at the age of 28 weeks. Importantly, transcriptome
325 analyses confirmed by qRT-PCR and western blotting showed that that the genes linked to renal
326 fibrosis and inflammatory of the above gene expression were reversed in GCK^{mut} mice fed with
327 HFD at the age of 60 weeks (**Fig. 6D-G, Fig. S5**). These findings suggest that the attenuation of
328 renal injury in GCK^{Mut} mice on a HFD at a young age may be correlated with the attenuation of
329 tissue lipid accumulation, fibrosis, and inflammatory responses.
330

331 **4. Discussion**

332 GCK-MODY is one of most common types of monogenic diabetes [29]. Patients with GCK-
333 MODY usually exhibit mild and asymptomatic fasting hyperglycemia, persisting from birth with
334 minimal progression over time [4-6]. Generally, the mild elevated blood glucose in GCK-MODY
335 does not require treatment with antidiabetic medications, except during pregnancy [30-32]. One
336 primary rationale for this lies in the markedly low incidence of microvascular and macrovascular
337 complications, nearly akin to those observed in healthy individuals [33, 34]. Previous studies
338 have revealed that patients with GCK-MODY showcase normal metabolic profiles, including
339 relatively lower serum TG with higher HDL-c levels, which may contribute to fewer
340 complications in these patients [35, 36]. However, given the fact that uncontrolled prolonged
341 hyperglycemia is strongly associated with diabetes complications and the lack of perspective
342 studies focusing on patients with GCK-MODY in different dietary settings, the long-term effects
343 of GCK inactivating mutations on chronic complications remain to be further determined.
344

345 In this study, using a newly established mouse model carrying a novel MODY causing GCK
346 mutation, we delved into the impact of the GCK mutant on lipid profiles and diabetic
347 complications from youth to old age, paying particular attention to a commonly overlooked
348 factors: the combination of mild hyperglycemia and a high-fat diet. We founded a reduction of
349 abnormal lipid profiles and mitigated renal injuries in 28-week-old GCK^{Mut} mice fed with HFD.
350 However, over an extended duration, a tendency towards exacerbated abnormalities in lipid
351 metabolism and heightened renal damage was observed (**Figs. 4-6**). These data revealed
352 surprisingly distinct duration and diet dependent effects of GCK^{Mut} and uncover previously
353 unrecognized pathological significance of prolonged reduction of GCK activity in lipid
354 metabolism and kidney injuries in patients with GCK-MODY. These data may be more
355 informative as controlled experimental variables can minimize complex clinical factors including
356 genetic diversity and use of different medications. These observations warrant further studies in
357 humans.
358
359 One of clinical features of patients with GCK-MODY is optimal lipid profile characterizing as
360 significantly lower levels of serum LDL-c and TG along with a higher level of HDL-c compared
361 with nondiabetic control and patients with T2D [24, 36]. A recent study reveals an increased
362 recruitment of adipose triglyceride lipase and choline/ethanolamine phosphotransferase 1 onto
363 the surface of HDLs, resulting in enhanced production of plasmalogen phosphatidylcholines that
364 may confer vascular protection against chronic exposure to hyperglycemia [35]. In this study, we
365 found that although there were decreased levels of serum LDL-c and TG, there were no
366 differences in serum HDL-c between control and GCK^{mut} fed with ND (**Fig. 1**). However, under
367 a metabolic stress (fed with HFD), GCK^{mut} exhibits more beneficial effects not only on levels of

368 HDL-c (**Fig. 4**), but also on renal lipid deposition and injuries (**Fig. 5**) at the age of 28 weeks.
369 These observations suggest that beneficial effects GCK^{mut} on lipid metabolism may override the
370 negative impacts of hyperglycemia on the renal damage at the early stages of diabetes. However,
371 as prolonged hyperglycemia further extends especially under the HFD conditions, these
372 beneficial lipid metabolisms were gradually reversed along with increased proteinuria and renal
373 injuries (**Figs. 2-3 and 5-6**). It remains to be determined whether these paradoxical duration and
374 diet dependent effects of GCK^{Mut} were solely due to extra long-term exposure of hyperglycemia
375 that directly disallows the protective effects of GCK^{Mut} on kidneys, or further prolonged
376 hyperglycemia rejects beneficial effects of GCK^{Mut} on lipid metabolism, resulting more severe
377 abnormal lipid profiles that may in turn damage kidney.
378
379 Recent studies have underscored the pivotal role of inflammation in the pathogenesis of DKD,
380 indicating its significance in triggering metabolic, biochemical, and hemodynamic disturbances
381 in diabetes [37, 38]. DKD, recognized as a chronic, low-grade inflammatory disease, represents a
382 primary feature associated with T2D and its microvascular complications [39-41]. Renal
383 inflammation manifests through immune cell infiltration, cytokine and chemokine release, and
384 activation of inflammatory signaling pathways [42]. Our investigation aligns with these findings,
385 demonstrating that 60-week-old GCK^{Mut} mice, both on a ND or HFD, exhibited more severe
386 renal inflammatory infiltration compared to controls (**Figs. 3 and 6**). Conversely, the observed
387 reduction in renal proteinuria and pathological changes in 28-week-old GCK^{Mut} mice fed with
388 HFD may be associated with diminished inflammatory infiltration. The characteristic
389 pathological hallmark linked with DKD involves the accumulation of extracellular matrix (ECM)
390 components in the glomeruli, often leading to renal angio-glomerulosclerosis and functional

391 decline [19-22]. Our study suggests that GCK^{Mut} may mitigate renal fibrosis by curbing ECM
392 accumulation and expansion of the thylakoid matrix in the early stages of diabetic nephropathy,
393 thereby substantially preserving renal function in diabetic mice. Additionally, previous research
394 has indicated that kidneys of mice on a HFD exhibited notable glomerular and tubular injury,
395 inclusive of substantial defects in the glomerular filtration barrier and heightened tubular cell
396 apoptosis [43, 44]. These effects were possibly linked to increased TC and TG content, alongside
397 activation of the adipogenic pathway in the kidneys [45, 46]. Correspondingly, our observations
398 reinforce these findings, indicating that this protective effect on the kidney wanes or even
399 exacerbates renal injury as the lipid profile deteriorates with prolonged high-fat feeding in
400 GCK^{Mut} mice.
401

402 **5. Conclusions**

403 In summary, our study presents novel evidence emphasizing the pivotal role of GCK in
404 glucolipid metabolism and the progression of diabetic complications. MODY causing GCK
405 mutant benefits lipid metabolism, decreasing renal lipid deposition, inflammatory infiltration,
406 and fibrosis progression in the early stages, thus retarding disease advancement. However, GCK
407 mutant appeared to be associated with exacerbated abnormalities of lipid metabolism and renal
408 injury in later stages. These distinct duration-dependent effects of GCK mutant raise the question
409 regarding current consensus for the management of patients with GCK-MODY.
410

411 **Declarations of interest**

412 The authors declare that no conflicts of interest exist and have no financial interests associated
413 with the present study.

414

415 **Data availability**

416 The authors are willing to make the raw data generated in their study available to other

417 investigators upon reasonable request.

418

419 **Funding**

420 The work was supported by the National Key R&D Program (2022YFE0131400 and

421 2019YFA0802502), and also by the National Natural Science Foundation of China

422 (82220108014, 82100865, and 82301951). We acknowledge the support of Tianjin Key Medical

423 Discipline (Specialty) Construction Project (TJYXZDXK-030A)， Tianjin Municipal Health

424 Commission (TJWJ2021ZD001), Tianjin Municipal Science and Technology Commission

425 (23JCQNJC00680), Tianjin Medical University General Hospital Clinical Research Program

426 (22ZYYLCZD02)， and Tianjin Medical University Clinical Special Disease Research Center -

427 Neuroendocrine Tumor Clinical Special Disease Research Center.

428

429

430 **Author contributions**

431 YH, YF, YF, XL, XL,WQ and YY conducted experiments and analyzed data; YL, WL, ZZ, SM,

432 SJ, SC, HS, KW and WF conducted experiments; QH discussed project and edited manuscript;

433 ML initiated and oversaw the project, designed the experiments, and wrote the manuscript.

434

435 **References**

436 [1] Matschinsky FM. Glucokinase as glucose sensor and metabolic signal generator in pancreatic
437 beta-cells and hepatocytes. Diabetes. 1990;39(6):647-52.
438 [2] Sternisha SM, and Miller BG. Molecular and cellular regulation of human glucokinase. Arch
439 Biochem Biophys. 2019;663:199-213.
440 [3] Bonnefond A, Unnikrishnan R, Doria A, Vaxillaire M, Kulkarni RN, Mohan V, et al.
441 Monogenic diabetes. Nat Rev Dis Primers. 2023;9(1):12.
442 [4] Pulst K, Arbo T, Kahre T, Peet A, and Tillmann V. MODY2 caused by a novel mutation of
443 GCK gene. J Pediatr Endocrinol Metab. 2012;25(7-8):801-3.
444 [5] Shields BM, Hicks S, Shepherd MH, Colclough K, Hattersley AT, and Ellard S. Maturity-
445 onset diabetes of the young (MODY): how many cases are we missing? Diabetologia.
446 2010;53(12):2504-8.
447 [6] Chakera AJ, Steele AM, Gloyn AL, Shepherd MH, Shields B, Ellard S, et al. Recognition and
448 Management of Individuals With Hyperglycemia Because of a Heterozygous Glucokinase
449 Mutation. Diabetes Care. 2015;38(7):1383-92.
450 [7] Hulín J, Škopková M, Valkovičová T, Mikulajová S, Rosoľanková M, Papcun P, et al.
451 Clinical implications of the glucokinase impaired function - GCK MODY today. Physiol Res.
452 2020;69(6):995-1011.
453 [8] Bishay RH, and Greenfield JR. A review of maturity onset diabetes of the young (MODY)
454 and challenges in the management of glucokinase-MODY. Med J Aust. 2016;205(10):480-5.
455 [9] Steele AM, Shields BM, Wensley KJ, Colclough K, Ellard S, and Hattersley AT. Prevalence
456 of vascular complications among patients with glucokinase mutations and prolonged, mild
457 hyperglycemia. Jama. 2014;311(3):279-86.

458 [10] Stride A, Shields B, Gill-Carey O, Chakera AJ, Colclough K, Ellard S, et al. Cross-sectional
459 and longitudinal studies suggest pharmacological treatment used in patients with glucokinase
460 mutations does not alter glycaemia. Diabetologia. 2014;57(1):54-6.
461 [11] Carmody D, Naylor RN, Bell CD, Berry S, Montgomery JT, Tadie EC, et al. GCK-MODY
462 in the US National Monogenic Diabetes Registry: frequently misdiagnosed and unnecessarily
463 treated. Acta Diabetol. 2016;53(5):703-8.
464 [12] Au SC, Tang SM, Rong SS, Chen LJ, and Yam JC. Association between hyperglycemia and
465 retinopathy of prematurity: a systemic review and meta-analysis. Sci Rep. 2015;5:9091.
466 [13] Nieves-Cintrón M, Flores-Tamez VA, Le T, Baudel MM, and Navedo MF. Cellular and
467 molecular effects of hyperglycemia on ion channels in vascular smooth muscle. Cell Mol Life
468 Sci. 2021;78(1):31-61.
469 [14] Tomlinson DR, and Gardiner NJ. Glucose neurotoxicity. Nat Rev Neurosci. 2008;9(1):36-45.
470 [15] Alicic RZ, Rooney MT, and Tuttle KR. Diabetic Kidney Disease: Challenges, Progress, and
471 Possibilities. Clin J Am Soc Nephrol. 2017;12(12):2032-45.
472 [16] Liu J, Fu H, Kang F, Ning G, Ni Q, Wang W, et al. β-Cell glucokinase expression was
473 increased in type 2 diabetes subjects with better glycemic control. J Diabetes. 2023;15(5):409-18.
474 [17] Beckman JA, and Creager MA. Vascular Complications of Diabetes. Circ Res.
475 2016;118(11):1771-85.
476 [18] Stumvoll M, Goldstein BJ, and van Haeften TW. Type 2 diabetes: principles of pathogenesis
477 and therapy. Lancet. 2005;365(9467):1333-46.
478 [19] Xue M, Sun H, Xu R, Wang Y, Guo J, Li X, et al. GADD45B Promotes Glucose-Induced
479 Renal Tubular Epithelial-Mesenchymal Transition and Apoptosis via the p38 MAPK and JNK
480 Signaling Pathways. Front Physiol. 2020;11:1074.

481 [20] Pan Y, Wang Y, Cai L, Cai Y, Hu J, Yu C, et al. Inhibition of high glucose-induced
482 inflammatory response and macrophage infiltration by a novel curcumin derivative prevents
483 renal injury in diabetic rats. Br J Pharmacol. 2012;166(3):1169-82.
484 [21] Wang S, Li Y, Fan J, Zhang X, Luan J, Bian Q, et al. Interleukin-22 ameliorated renal injury
485 and fibrosis in diabetic nephropathy through inhibition of NLRP3 inflammasome activation. Cell
486 Death Dis. 2017;8(7):e2937.
487 [22] Chang YP, Sun B, Han Z, Han F, Hu SL, Li XY, et al. Saxagliptin Attenuates Albuminuria
488 by Inhibiting Podocyte Epithelial- to-Mesenchymal Transition via SDF-1α in Diabetic
489 Nephropathy. Front Pharmacol. 2017;8:780.
490 [23] Xie Z, Xie T, Liu J, Zhang Q, and Xiao X. Glucokinase Inactivation Ameliorates Lipid
491 Accumulation and Exerts Favorable Effects on Lipid Metabolism in Hepatocytes. Int J Mol Sci.
492 2023;24(5).
493 [24] Ping F, Fu J, and Xiao X. Distinguishing the lipid profile of GCK-MODY patients and its
494 correlation with hsCRP levels. Front Endocrinol (Lausanne). 2022;13:1024431.
495 [25] Fendler W, Rizzo M, Borowiec M, Malachowska B, Antosik K, Szadkowska A, et al. Less
496 but better: cardioprotective lipid profile of patients with GCK-MODY despite lower HDL
497 cholesterol level. Acta Diabetol. 2014;51(4):625-32.
498 [26] D'Agati VD, Chagnac A, de Vries AP, Levi M, Porrini E, Herman-Edelstein M, et al.
499 Obesity-related glomerulopathy: clinical and pathologic characteristics and pathogenesis. Nat
500 Rev Nephrol. 2016;12(8):453-71.
501 [27] Xiong W, Xiong Z, Song A, Lei C, Ye C, and Zhang C. Relieving lipid accumulation
502 through UCP1 suppresses the progression of acute kidney injury by promoting the
503 AMPK/ULK1/autophagy pathway. Theranostics. 2021;11(10):4637-54.

504 [28] Chen J, Li T, Vladmir C, Yuan Y, and Sun Z. Renal lipid accumulation induced by high-fat
505 diet regulates glucose homeostasis via sodium-glucose cotransporter 2. Diabetes Res Clin Pract.
506 2021;179:109027.
507 [29] Anık A, Çatlı G, Abacı A, and Böber E. Maturity-onset diabetes of the young (MODY): an
508 update. J Pediatr Endocrinol Metab. 2015;28(3-4):251-63.
509 [30] Timsit J, Ciangura C, Dubois-Laforgue D, Saint-Martin C, and Bellanne-Chantelot C.
510 Pregnancy in Women With Monogenic Diabetes due to Pathogenic Variants of the Glucokinase
511 Gene: Lessons and Challenges. Front Endocrinol (Lausanne). 2021;12:802423.
512 [31] Urakami T. Maturity-onset diabetes of the young (MODY): current perspectives on
513 diagnosis and treatment. Diabetes Metab Syndr Obes. 2019;12:1047-56.
514 [32] Tosur M, and Philipson LH. Precision diabetes: Lessons learned from maturity-onset
515 diabetes of the young (MODY). J Diabetes Investig. 2022;13(9):1465-71.
516 [33] Hattersley AT, Greeley SAW, Polak M, Rubio-Cabezas O, Njølstad PR, Mlynarski W, et al.
517 ISPAD Clinical Practice Consensus Guidelines 2018: The diagnosis and management of
518 monogenic diabetes in children and adolescents. Pediatr Diabetes. 2018;19 Suppl 27:47-63.
519 [34] Gloyn AL. Glucokinase (GCK) mutations in hyper- and hypoglycemia: maturity-onset
520 diabetes of the young, permanent neonatal diabetes, and hyperinsulinemia of infancy. Hum
521 Mutat. 2003;22(5):353-62.
522 [35] Wang X, Lam SM, Cao M, Wang T, Wang Z, Yu M, et al. Localized increases in CEPT1 and
523 ATGL elevate plasmalogen phosphatidylcholines in HDLs contributing to atheroprotective lipid
524 profiles in hyperglycemic GCK-MODY. Redox Biol. 2021;40:101855.

525 [36] Spégel P, Ekholm E, Tuomi T, Groop L, Mulder H, and Filipsson K. Metabolite profiling
526 reveals normal metabolic control in carriers of mutations in the glucokinase gene (MODY2).
527 Diabetes. 2013;62(2):653-61.
528 [37] Pérez-Morales RE, Del Pino MD, Valdivielso JM, Ortiz A, Mora-Fernández C, and
529 Navarro-González JF. Inflammation in Diabetic Kidney Disease. Nephron. 2019;143(1):12-6.
530 [38] Rayego-Mateos S, Rodrigues-Diez RR, Fernandez-Fernandez B, Mora-Fernández C,
531 Marchant V, Donate-Correa J, et al. Targeting inflammation to treat diabetic kidney disease: the
532 road to 2030. Kidney Int. 2023;103(2):282-96.
533 [39] Bonner R, Albajrami O, Hudspeth J, and Upadhyay A. Diabetic Kidney Disease. Prim Care.
534 2020;47(4):645-59.
535 [40] Jung CY, and Yoo TH. Pathophysiologic Mechanisms and Potential Biomarkers in Diabetic
536 Kidney Disease. Diabetes Metab J. 2022;46(2):181-97.
537 [41] Lin YC, Chang YH, Yang SY, Wu KD, and Chu TS. Update of pathophysiology and
538 management of diabetic kidney disease. J Formos Med Assoc. 2018;117(8):662-75.
539 [42] Winiarska A, Knysak M, Nabrdalik K, Gumprecht J, and Stompór T. Inflammation and
540 Oxidative Stress in Diabetic Kidney Disease: The Targets for SGLT2 Inhibitors and GLP-1
541 Receptor Agonists. Int J Mol Sci. 2021;22(19).
542 [43] Yamamoto T, Takabatake Y, Takahashi A, Kimura T, Namba T, Matsuda J, et al. High-Fat
543 Diet-Induced Lysosomal Dysfunction and Impaired Autophagic Flux Contribute to Lipotoxicity
544 in the Kidney. J Am Soc Nephrol. 2017;28(5):1534-51.
545 [44] Nakamura J, Yamamoto T, Takabatake Y, Namba-Hamano T, Minami S, Takahashi A, et al.
546 TFEB-mediated lysosomal exocytosis alleviates high-fat diet-induced lipotoxicity in the kidney.
547 JCI Insight. 2023;8(4).

[45] de Vries AP, Ruggenenti P, Ruan XZ, Praga M, Cruzado JM, Bajema IM, et al. Fatty kidney: emerging role of ectopic lipid in obesity-related renal disease. Lancet Diabetes Endocrinol. 2014;2(5):417-26.

[46] Chen Y, Deb DK, Fu X, Yi B, Liang Y, Du J, et al. ATP-citrate lyase is an epigenetic regulator to promote obesity-related kidney injury. Faseb j. 2019;33(8):9602-15.

571 **Figure 1**

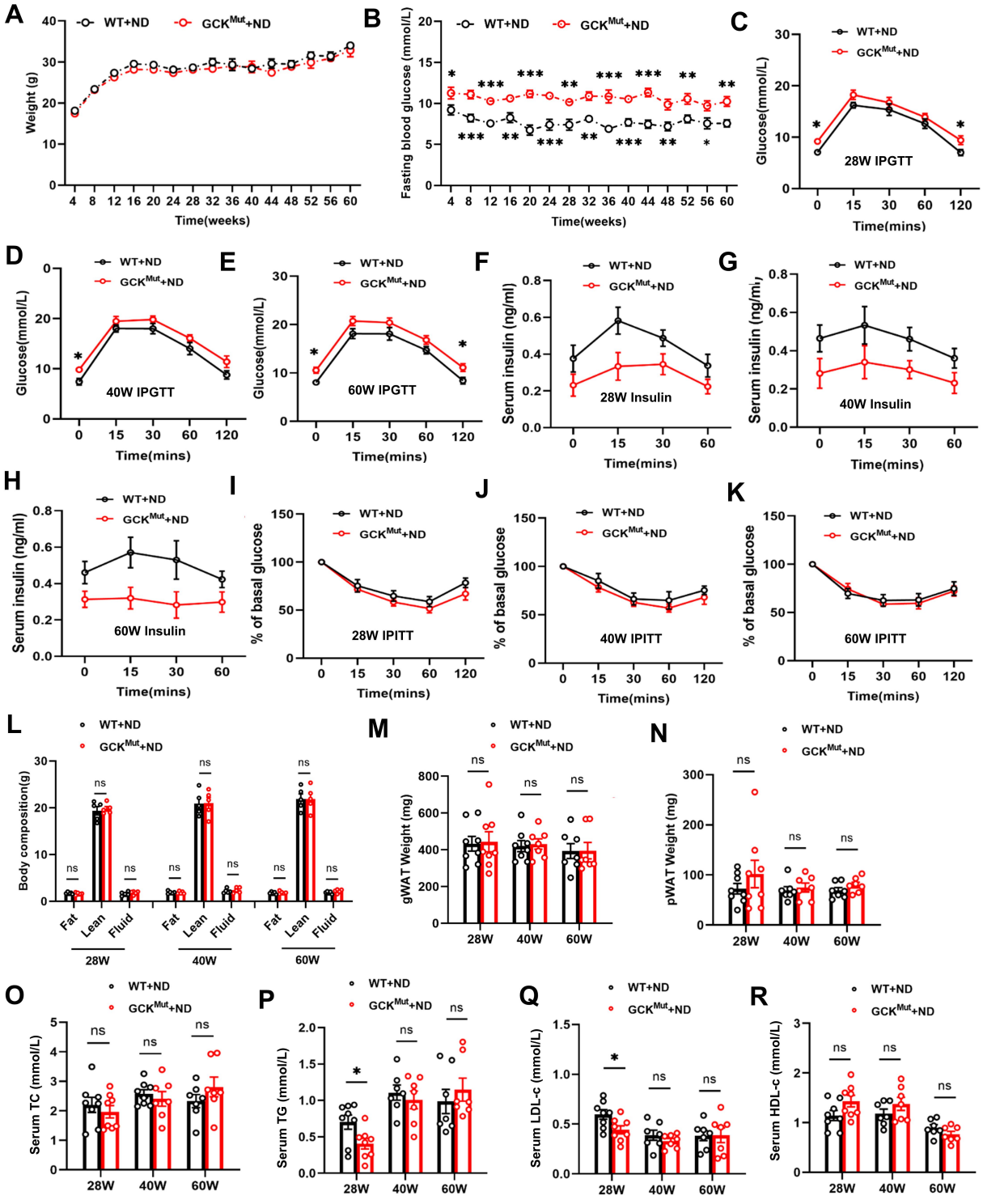

572

573 **Figure 1. GCK^{Mut} mice had elevated FBG but improved lipids.** Body weight (**A**) and fasting

574 blood glucose (**B**) were monitored every 4 weeks (n=7-8 mice/group). (**C-E**) Two groups of

575 mice were intraperitoneally injected with 1 g/kg for IPGTT at 28, 40, or 60 weeks of age
576 (n=5mice/group). (**F-H**) Serum insulin levels were measured by ELISA during IPGTT in both
577 groups of mice (n=5 mice/group). (**I-K**) Two groups of mice were subjected to IPITT
578 (intraperitoneal injection of 0.75 U/kg, n=5mice/group) at 28, 40, or 60 weeks of age. (**L**) Body
579 composition analysis of both groups of mice using a body fat analyzer. (**M-N**) Wet weights of
580 fresh pWAT and gWAT of mice were measured at 28, 40, and 60 weeks of age. Blood samples
581 were used to measure lipid levels including TC (**O**), TG (**P**), LDL-c (**Q**), and HDL-c (**R**), n=5-
582 8mice/group. Values are expressed as mean±SEM. WT+ND vs. GCK^{Mut}+ND: *P<0.05,
583 **P<0.01, ***P<0.001, ns, not significant.
584
585
586
587
588
589
590
591
592
593
594
595
596
597

598 **Figure 2**

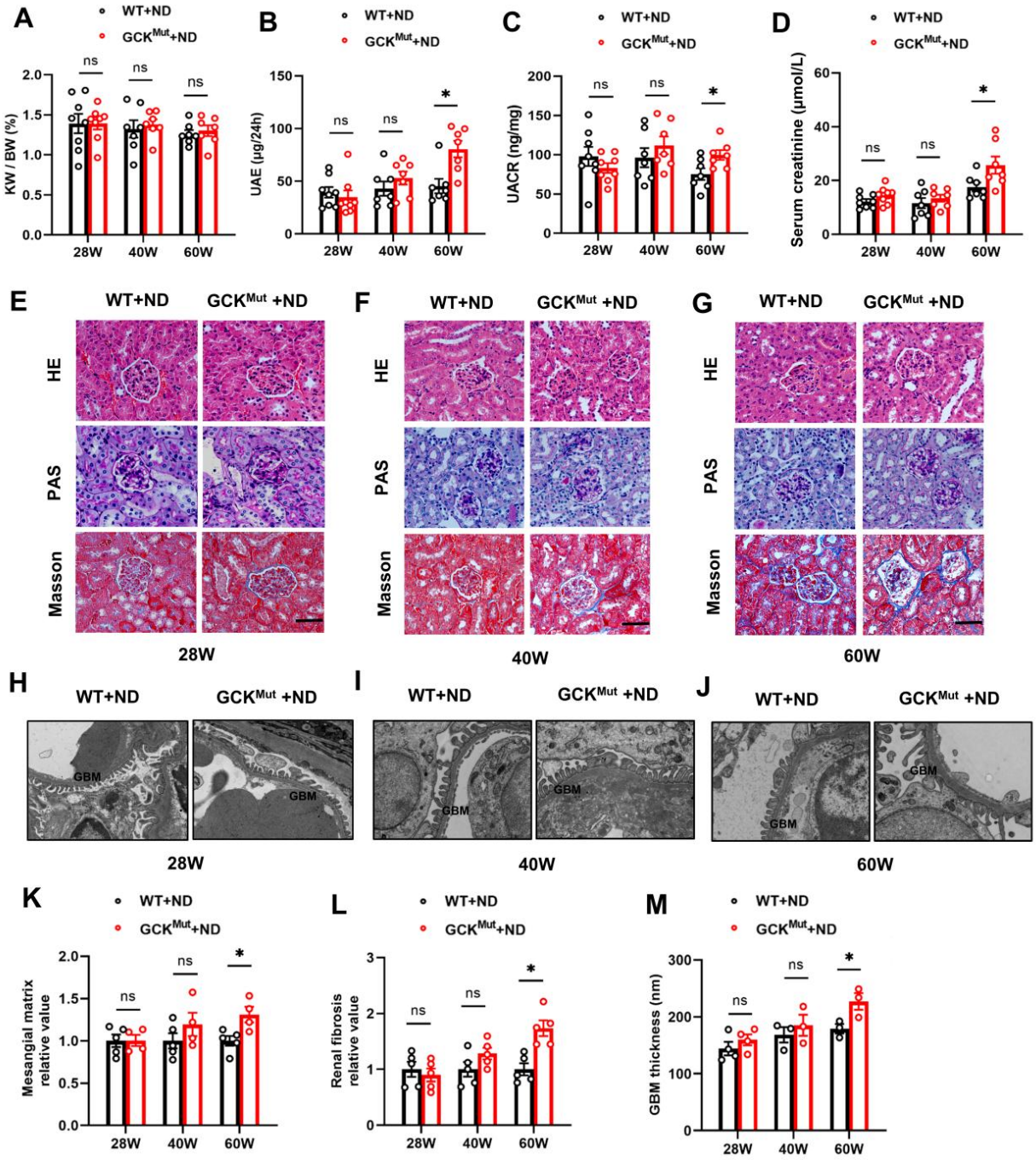

599

600 **Figure 2. Changes in UAE, serum creatinine and renal histology in GCK^{Mut} mice fed with**

601 **ND.** (**A**) Kidney and body weights were measured at 28, 40, 60-week old, the ratio of kidney and

602 bodyweight (KW/BW) were calculated. 24-hour UAE (**B**), UACR (**C**), and blood creatinine

603 levels (**D**) were examined in two groups of mice fed with ND at 28, 40, and 60 weeks of age
604 (n=7-8 mice/group). (**E-G**) H&E staining, PAS staining, and Masson staining of kidney sections
605 were performed at 28, 40, and 60 weeks in mice fed with ND (n=5 mice/group). Original
606 magnification = 400. Scale bar = 50μm. (**H-J**) Changes in glomerular structure observed by
607 electron microscopy (n=3 mice/group). Original magnification is x8k. Semi-quantitative analysis
608 of the mesangial matrix (**K**) and the degree of renal fibrosis (**L**). (**M**) Quantification of GBM
609 thickness. Values are expressed as mean±SEM. WT+ND vs. GCK^{Mut}+ND: *P<0.05, ns, not
610 significant.
611
612
613
614
615
616
617
618
619
620
621
622
623
624
625

Figure 3

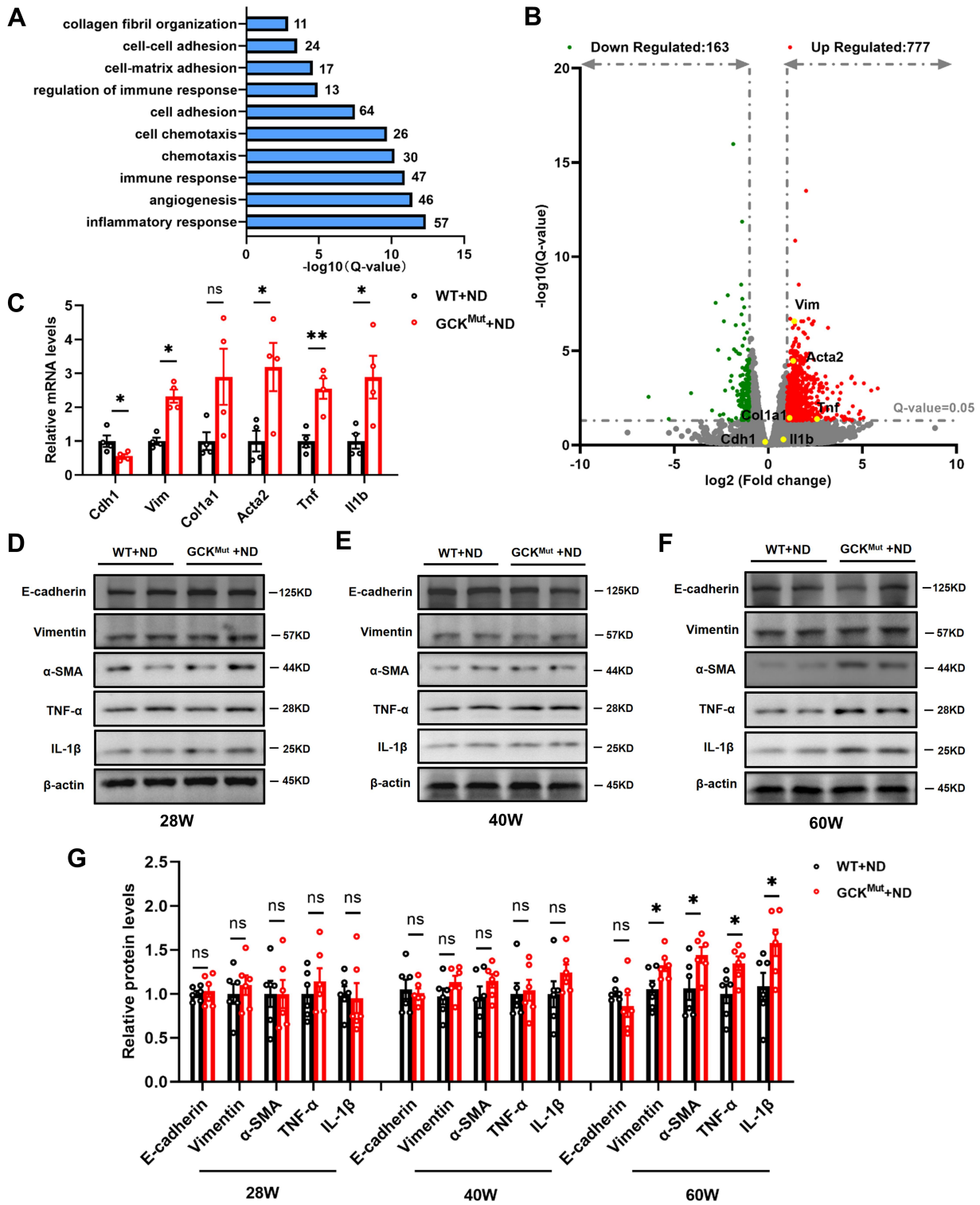
A
collagen fibril organization
cell-cell adhesion
cell-matrix adhesion
regulation of immune response
cell adhesion
cell chemotaxis
chemotaxis
immune response
angiogenesis
inflammatory response
11
24
17
13
64
26
30
47
46
57
-log10（Q-value）
B
Down Regulated:163
Up Regulated:777
-log10(Q-value)
log2 (Fold change)
Vim
Acta2
Tnf
Col1a1
Cdh1
Il1b
Q-value=0.05
C
Relative mRNA levels
WT+ND
GCK^Mut+ND
Cdh1
Vim
Col1a1
Acta2
Tnf
Il1b
D
E
F
WT+ND
GCK^Mut +ND
E-cadherin
Vimentin
α-SMA
TNF-α
IL-1β
β-actin
125KD
57KD
44KD
28KD
25KD
45KD
28W
40W
60W
G
Relative protein levels
WT+ND
GCK^Mut+ND
E-cadherin
Vimentin
α-SMA
TNF-α
IL-1β
28W
40W
60W

628 **Figure 3. Increased renal fibrosis and inflammatory infiltration in 60-week-old GCK^{Mut}**
629 **mice fed with ND.** (**A**) GO analysis of RNA-seq data showed significant changes of pathways in
630 the renal from 60-week-old WT control and GCK^{Mut} mice fed with ND (n=3mice/group). (**B**)
631 Volcano plots depicting transcriptome data, dashed line on the y-axis indicates Q-value=0.05 and
632 fold change on the x-axis is greater than 1. (**C**) The mRNA levels of indicated genes in the
633 kidneys of 60-week-old WT control and GCK^{Mut} mice were determined by qRT-PCR (n=4
634 mice/group). (**D-F**) At 28, 40, and 60 weeks of age, the expression of E-Cadherin, Vimentin, α-
635 SMA, TNF-α, and IL-1β in kidneys of control and GCK^{Mut} mice fed with ND were examined by
636 western blots (n=6 mice/group). (**G**) Quantification of western blots shown in D-F. Values are
637 expressed as mean±SEM. WT+ND vs. GCK^{Mut}+ND: *P<0.05, **P<0.01, ns, not significant.
638
639
640
641
642
643
644
645
646
647
648
649
650

651

Figure 4

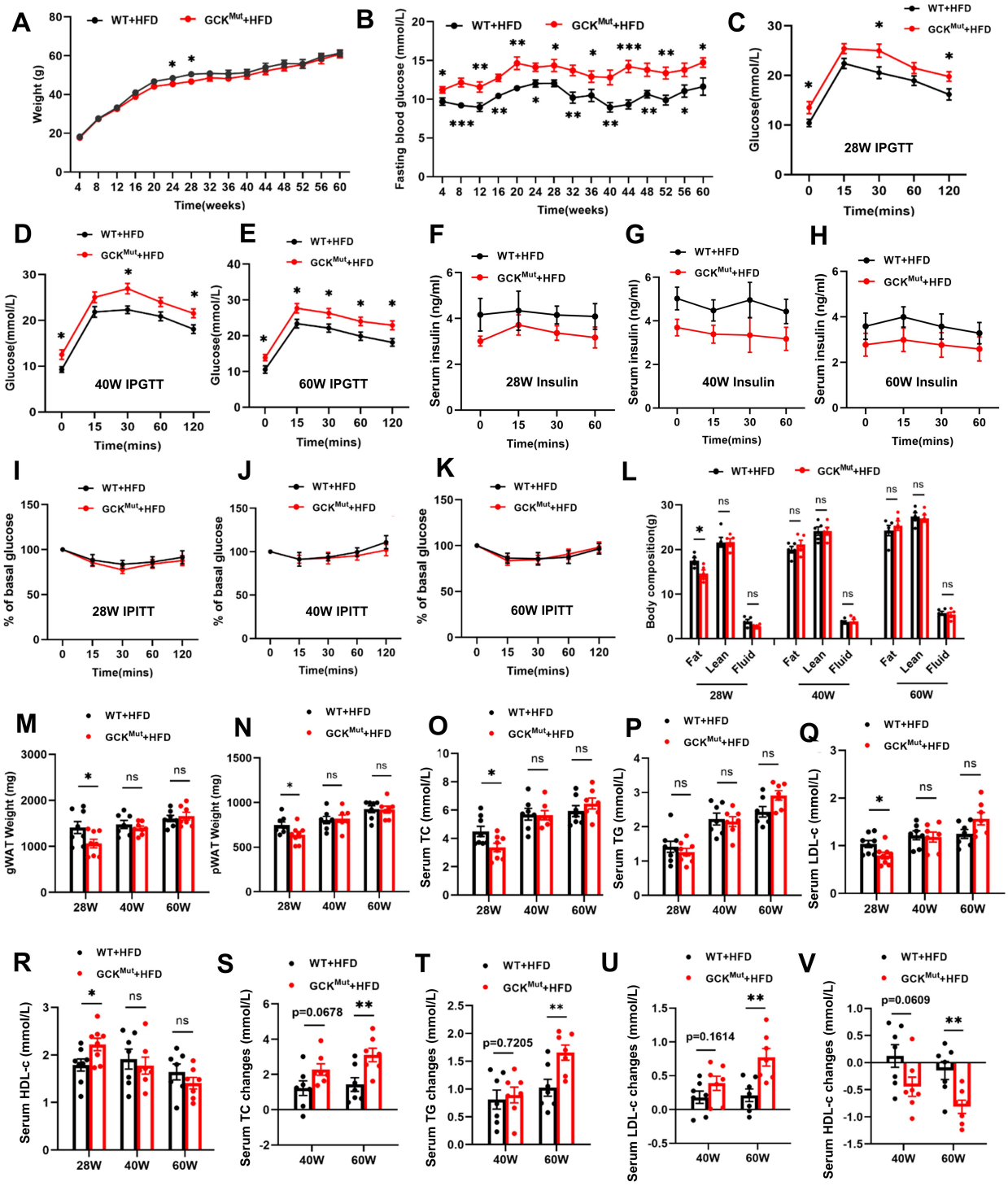

652

653 **Figure 4. Changes in FBG and lipid metabolism in GCK^{Mut} mice fed with HFD.** GCK^{Mut} and
654 control mice were fed with HFD started from 4 weeks of age. The body weight (**A**) and FBG (**B**)
655 have been monthly monitored and recorded till 60 weeks of age. IPGTT were performed in mice
656 fed with HFD at 28 (**C**), 40 (**D**), and 60 (**E**) weeks of age. Serum insulin levels during IPGTT
657 were also measured at 28 (**F**), 40 (**G**), and 60 (**H**) weeks of age. IPITT were performed in mice
658 fed with HFD at 28 (**I**), 40 (**J**), and 60 (**K**) weeks of age (n=5-8 mice/group). (**L**) Body
659 compositions were analyzed in the mice fed with HFD at 28, 40, and 60 weeks of age. (**M-N**)
660 The weight of pWAT and gWAT were measured in the mice above. TC (**O**), TG (**P**), LDL-c (**Q**),
661 HDL-c (**R**) were measured in the mice fed with HFD at 28, 40, and 60 weeks of age. (**S-V**)
662 Changes of TC, TG, LDL-c, HDL-c in mice aged 40 weeks and 60 weeks compared with those
663 aged 28 weeks. n=5-8 mice/group. Values were expressed as mean±SEM. WT+HFD vs.
664 GCK^{Mut}+HFD: *P<0.05, **P<0.01, ***P<0.001, ns, not significant.

665
666
667
668
669
670
671
672
673
674
675
676
677
678

Figure 5

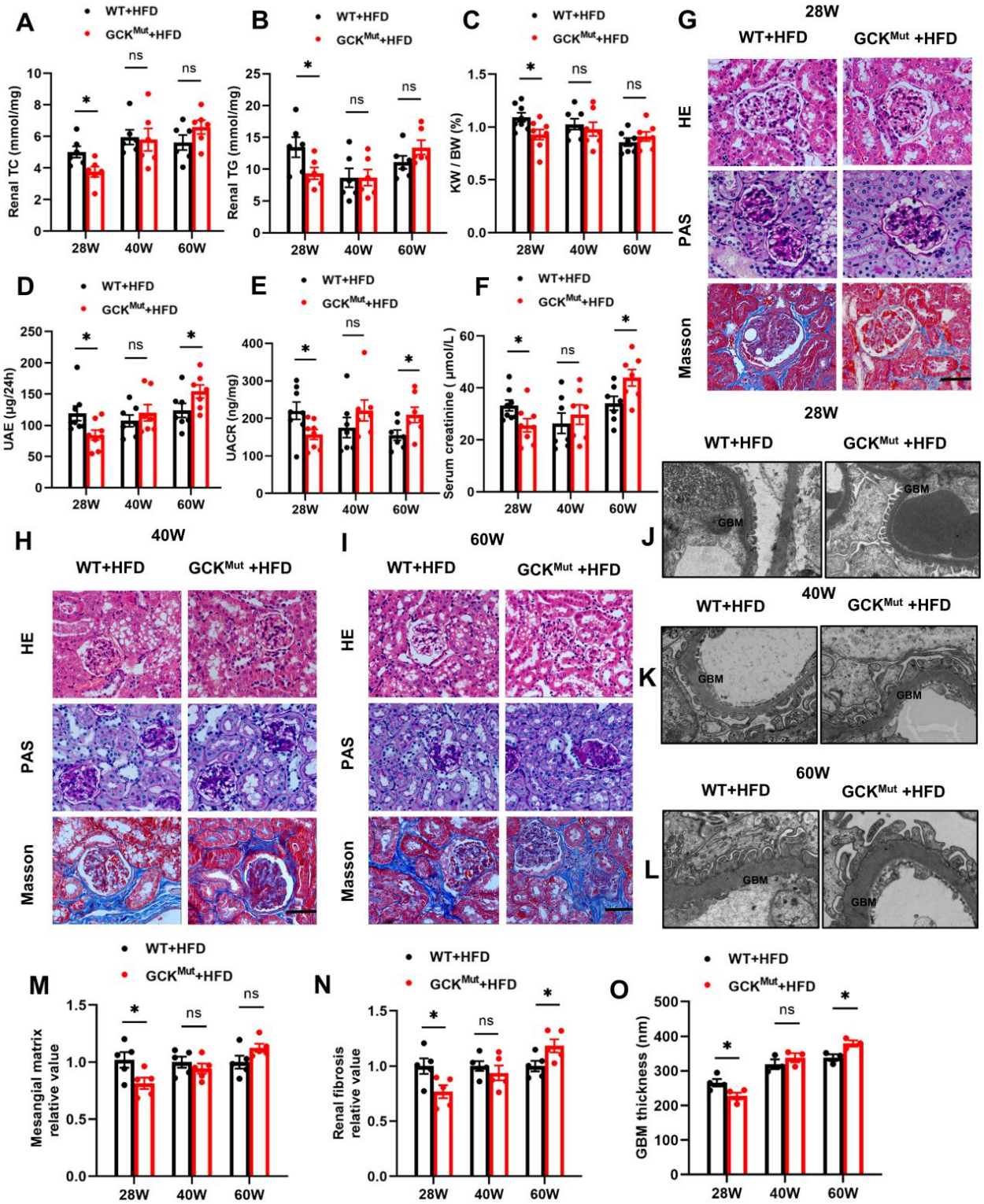
A
B
C
D
E
F
G
H
I
J
K
L
M
N
O
WT+HFD
GCK^Mut+HFD
Renal TC (mmol/mg)
Renal TG (mmol/mg)
KW / BW (%)
UAE (μg/24h)
UACR (ng/mg)
Serum creatinine (μmol/L)
Mesangial matrix relative value
Renal fibrosis relative value
GBM thickness (nm)
28W
40W
60W
ns
HE
PAS
Masson
GBM

680

681 **Figure 5. GCK^{Mut} attenuated HFD associated renal injury at 28 weeks of age, but**
682 **aggravated renal injury at 60 weeks of age.** Renal TC (**A**), Renal TG (**B**), KW/BW (**C**), 24-
683 hour UAE (**D**), UACR (**E**), and serum creatinine levels (**F**) were examined at 28, 40, and 60
684 weeks of age in both groups of mice (n=7-8 mice/group). (**G-I**) H&E staining, PAS staining, and
685 Masson staining of renal sections at 28, 40, and 60 weeks in both groups of mice (n=5
686 mice/group). Original magnification = 400. Scale bar = 50μm. (**J-L**) Electron microscopic
687 observation of changes in glomerular structure in two groups of mice (n=3 mice/group). Original
688 magnification is x8k. Semi-quantitative analysis of the mesangial matrix (**M**) and the degree of
689 renal fibrosis (**N**). Quantification of GBM thickness (**O**). Values are expressed as mean±SEM.
690 WT+HFD vs. GCK^{Mut}+HFD: *P<0.05, ns, not significant.
691
692
693
694
695
696
697
698
699
700
701
702
703

704

Figure 6

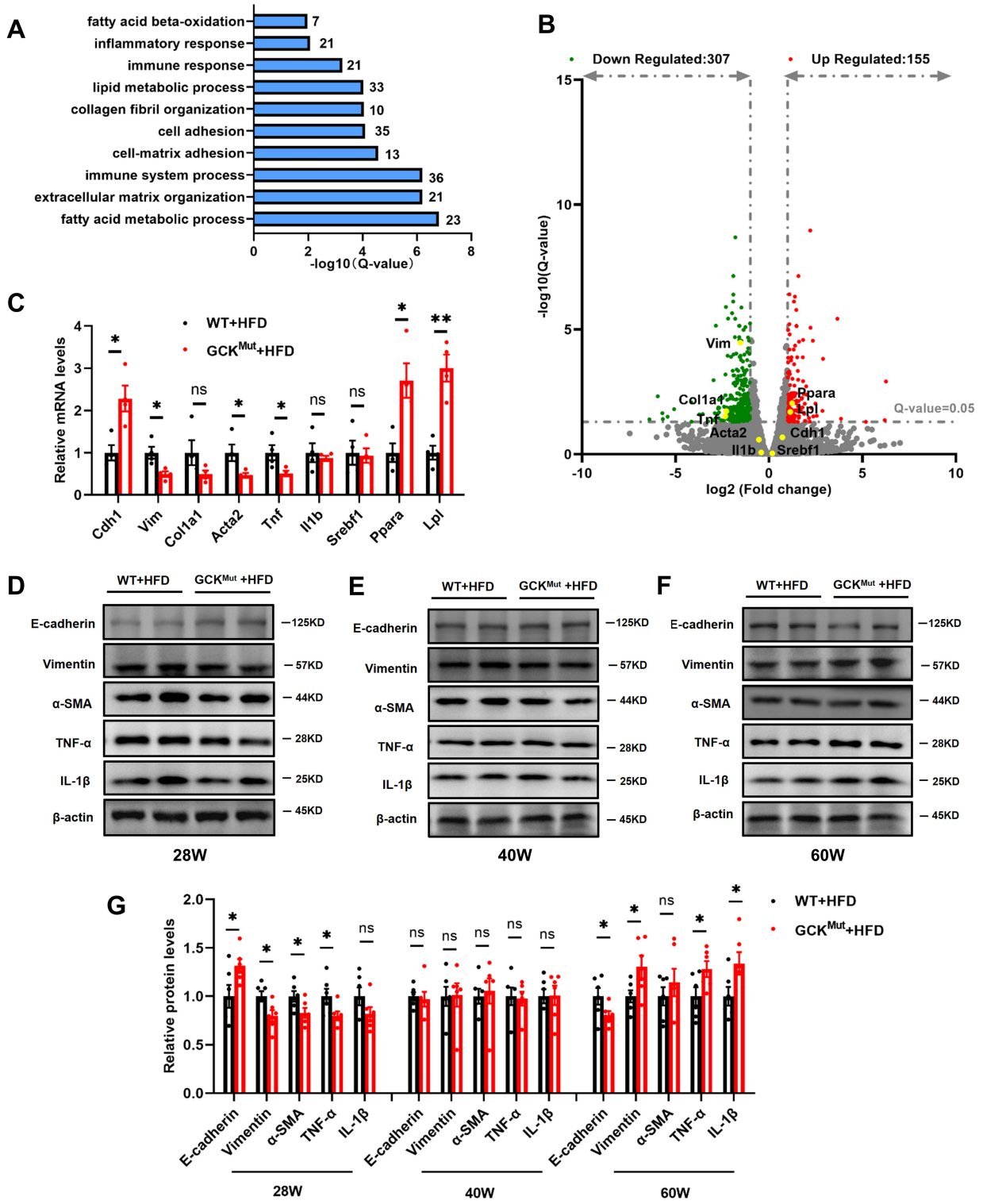

705

706 **Figure 6. Renal fibrosis and inflammatory were attenuated in HFD GCK^{Mut} mice at 28**
707 **weeks of age and aggravated at 60 weeks of age**. (**A**) The GO analysis of data obtained by
708 RNA-Seq showed significantly different gene enrichment (n=3 mice/group). (**B**) Volcano plots
709 depicting transcriptomics data, dashed line on the y-axis indicates Q-value=0.05 and fold change
710 on the x-axis is greater than 1. (**C**) The mRNA levels of the mentioned factors in the kidneys of
711 28-week-old HFD WT control and GCK^{Mut} mice were determined by qRT-PCR (n=4
712 mice/group). (**D-F**) Renal E-Cadherin, Vimentin, α-SMA, TNF-α, and IL-1β protein levels were
713 detected by Western blot analysis at 28, 40, and 60 weeks of age (n=6 mice/group). (**G**) Results
714 of quantitative immunoblot analysis for each group. Values are expressed as mean±SEM.
715 WT+HFD vs. GCK^{Mut}+HFD: *P<0.05, **P<0.01, ***P<0.001, ns, not significant.
716
717
718
719
720
721
722
723
724
725
726
727
728

729 **Supplemental Figure 1**

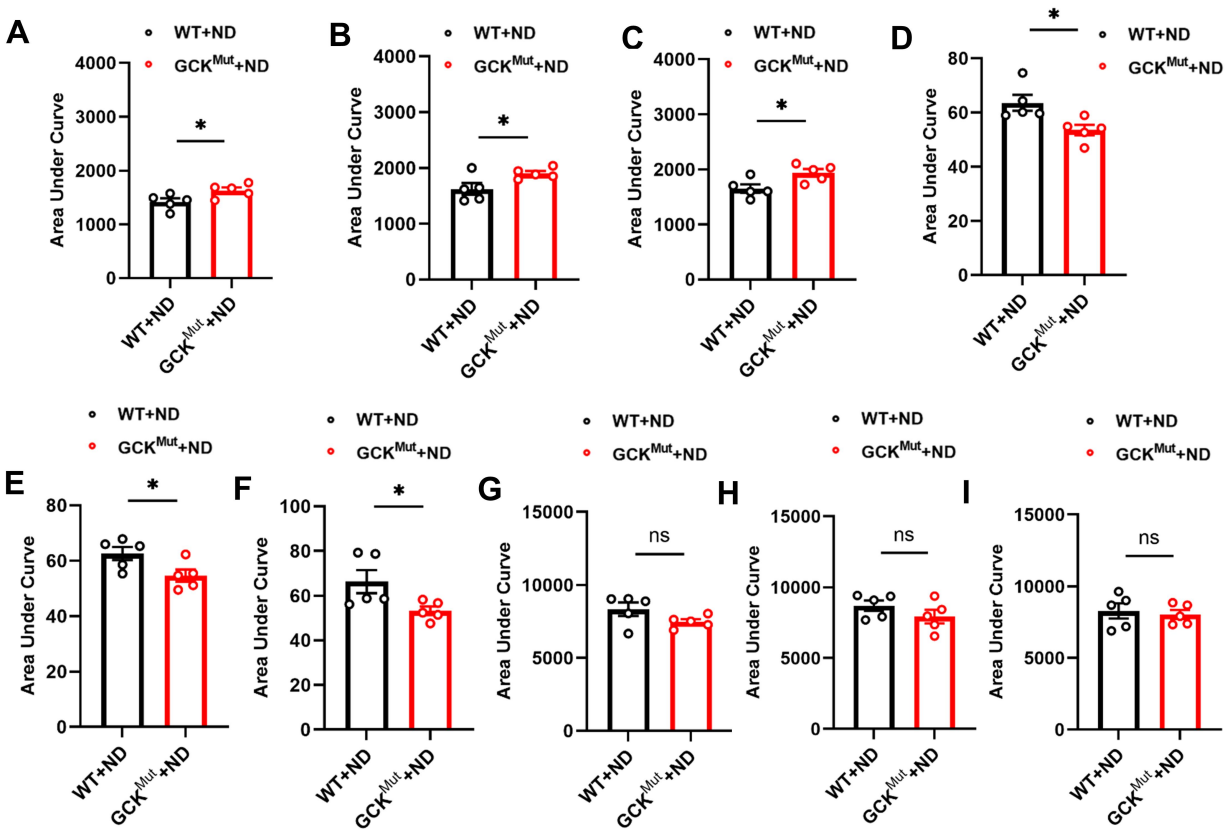

730

731 **Supplemental Figure 1. The area under the curve (AUC) of IPGTT, serum insulin and**

732 **IPITT in two groups of mice on ND.** (**A-C**) The AUCs of blood glucose levels were calculated

733 according to Fig.1C-E. (**D-F**) The AUCs of serum insulin levels were calculated from Fig. 1F-H.

734 (**G-I**) The AUCs of blood glucose during IPITT were calculated from Fig.1I-K. n=5mice/group.

735 Values are expressed as mean±SEM. WT+ND vs. GCK^{Mut}+ND: *P<0.05, ns, not significant.

736

737

738

739

740

741 **Supplemental Figure 2**

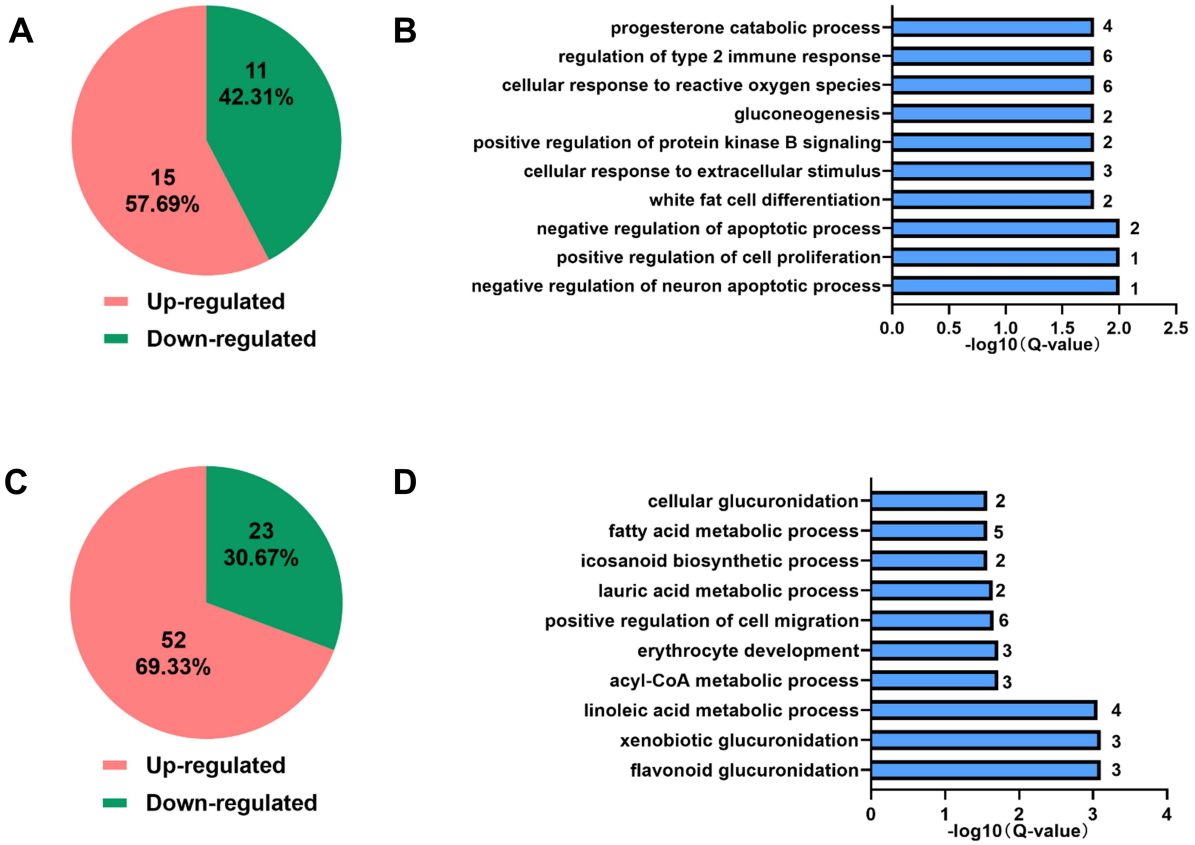

742

743 **Supplemental Figure 2. The kidney transcriptome analysis at 28 and 40 weeks in two**
744 **groups of mice on ND.** (**A-B**) The number of significantly different genes up- and down-
745 regulated and GO analysis in two groups of mice on regular diet at 28 weeks of age. (**C-D**) The
746 number of significantly different genes up- and down-regulated and GO analysis in two groups
747 of mice on ND at 40 weeks of age. n=3 mice/group.

748

749

750

751

752

753 **Supplemental Figure 3**

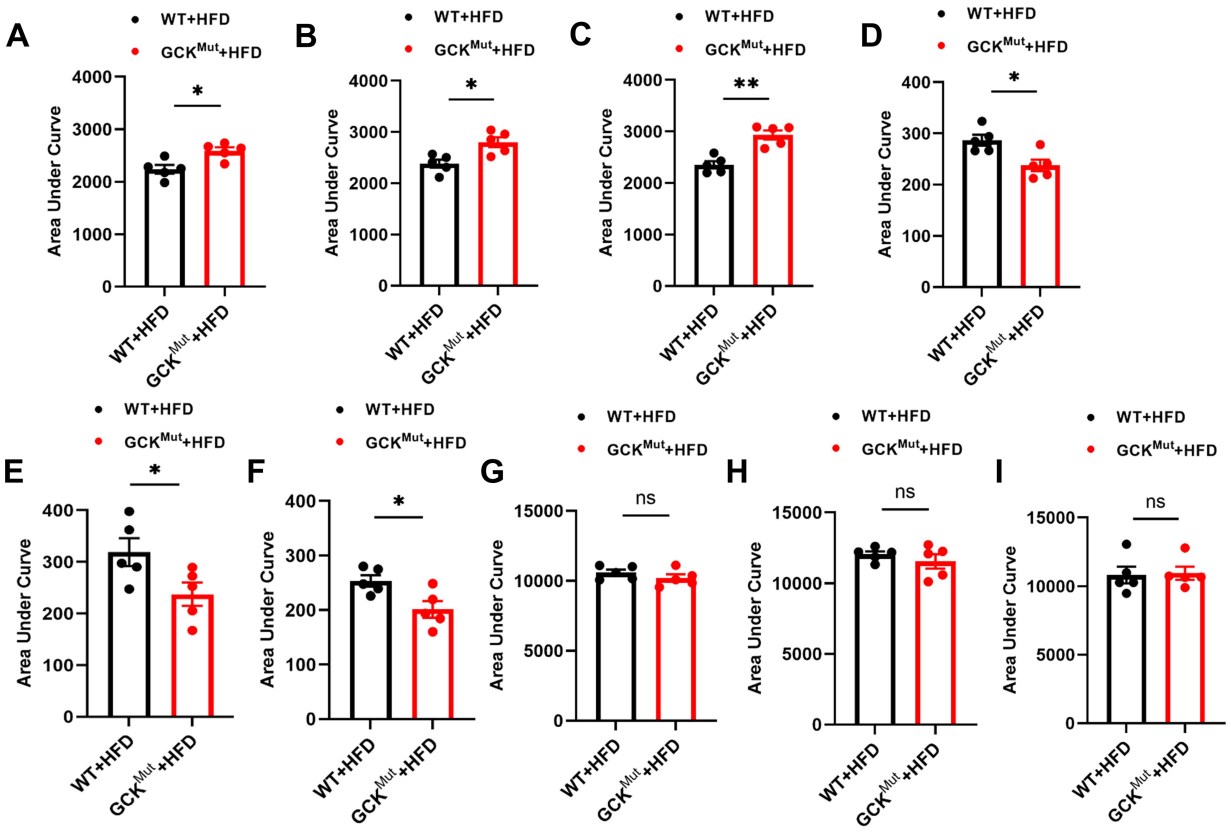

754

755 **Supplemental Figure 3. The area under the curve (AUC) of IPGTT, serum insulin, and**

756 **IPITT in two groups of mice fed with HFD.** (**A-C**) The AUC of IPGTT was calculated

757 according to Figure.5C-E. (**D-F**) The AUC for serum insulin levels was calculated from

758 Figure.5F-H. (**G-I**) The AUC values for IPITT were calculated from Figure.5I-K. n=5

759 mice/group. Values are expressed as mean±SEM. WT+HFD vs. GCK^{Mut}+HFD: *P<0.05, ns, not

760 significant.

761

762

763

764

765

766 **Supplemental Figure 4**

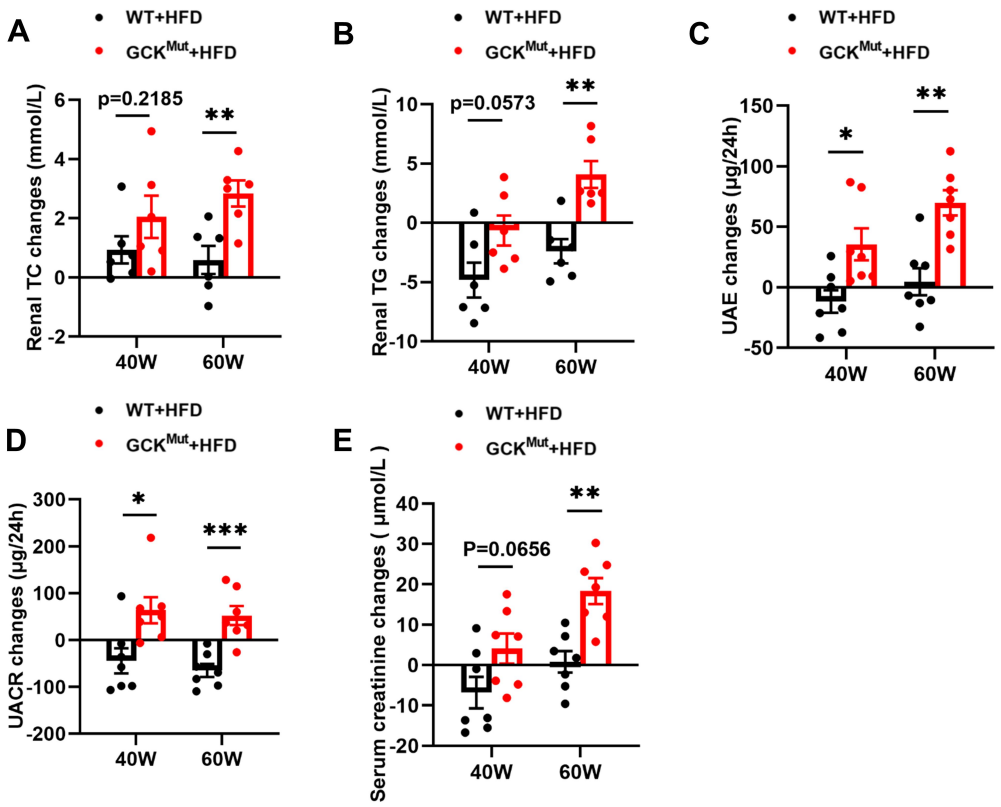

767

768 **Supplemental Figure 4. Changes of Renal TC, Renal TG, 24-hour UAE, UACR, and serum**
769 **creatinine in mice aged 40 weeks and 60 weeks compared with those aged 28 weeks fed with**
770 **HFD.** Changes of Renal TC (**A**), Renal TG (**B**), 24-hour UAE (**C**), UACR (**D**), and serum
771 creatinine (**E**) in mice aged 40 weeks and 60 weeks compared with those aged 28 weeks. Values
772 were expressed as mean±SEM. WT+HFD vs. GCK^{Mut}+HFD: *P<0.05, **P<0.01, ***P<0.001,
773 ns, not significant.

774

775

776

777

778

Supplemental Figure 5

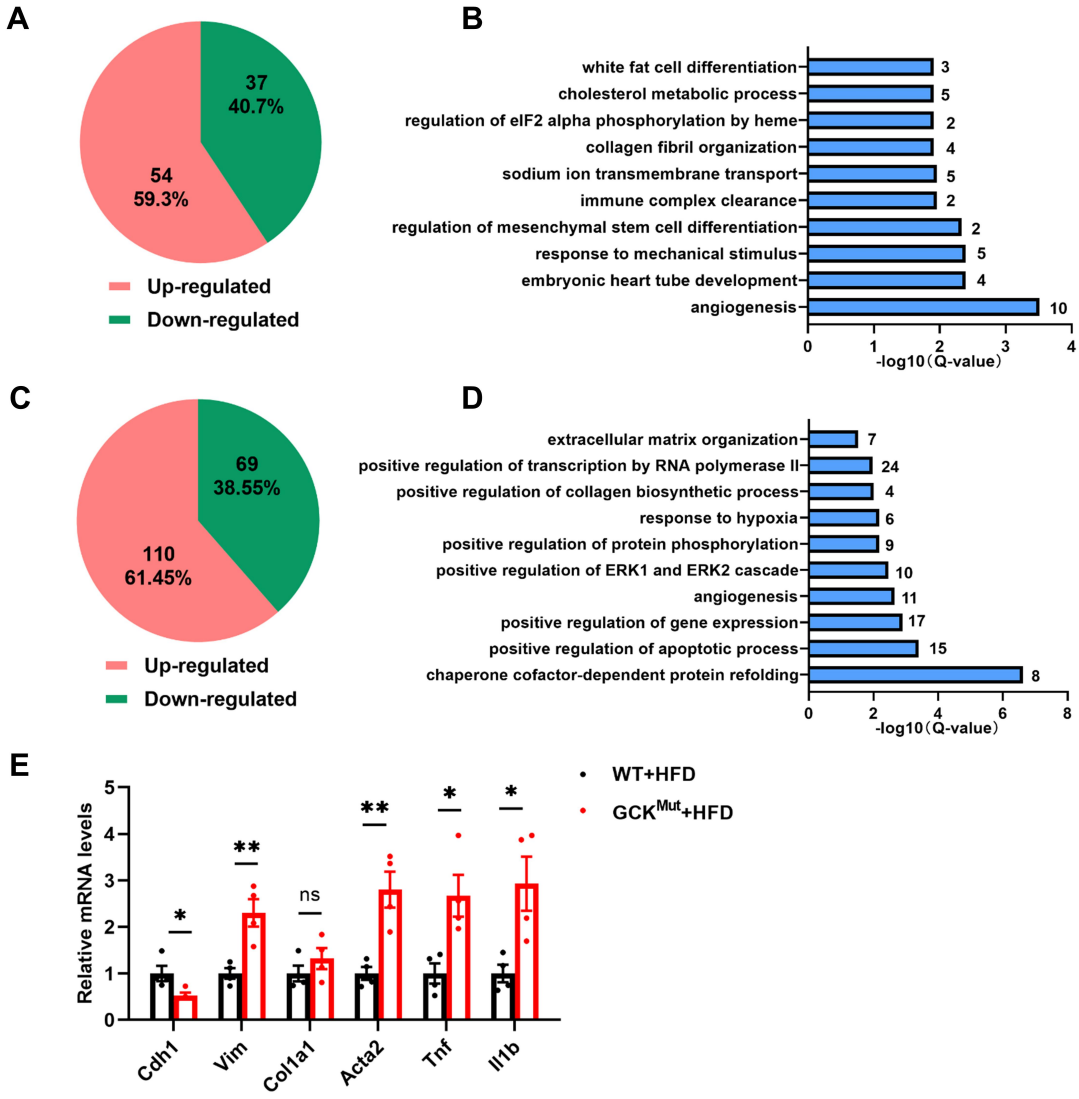

Supplemental Figure 5. The kidney transcriptome analysis at 40 and 60 weeks in two groups of mice on HFD. (**A-B**) The number of significantly different genes up- and down-regulated and GO analysis in two groups of mice on HFD at 40 weeks of age. (**C-D**) The number of significantly different genes up- and down-regulated and GO analysis in two groups of mice

787 on HFD at 60 weeks of age. (**E**) The mRNA levels of relevant fibrosis and inflammatory factors

788 in the kidneys of two groups of mice on HFD at 60 weeks of age.

789

790

Supplemental Table 1. Primer sequences (m-Mus musculus) for qRT-PCR (5'-3')

Gene	Forward	Reverse
mCdh1	CAGGTCTCCTCATGGCTTTGC	CTTCCGAAAAGAAGGCTGTCC
mVim	CGGCTGCGAGAGAAATTGC	CCACTTTCCGTTCAAGGTCAAG
mCol1a1	ATGTTCAGCTTTGTGGACCTC	CAGAAAGCACAGCACTCGC
mActa2	GTCCCAGACATCAGGGAGTAA	TCGGATACTTCAGCGTCAGGA
mTNF-α	GCGACGTGGAACTGGCAGAAGAGG	GTACTTGGGCAGATTGACCTCAGC
mIL-1β	CACTACAGGCTCCGAGATGAACAAC	TGTCGTTGCTTGGTTCTCCTTGTAC
mSrebf1	GGAGCCATGGATTGCACATT	GGCCCGGGAAGTCACTGT
mPpara	AGAGCCCCATCTGTCCTCTC	ACTGGTAGTCTGCAAAACCAAA
mLpl	GGGAGTTTGGCTCCAGAGTTT	TGTGTCTTCAGGGGTCCTTAG
mGAPDH	ACCCACTCCTCCACCTTTGAC	TGTTGCTGTAGCCAAATTCGTT

791

792